# Zero-Oscillation Adaptive-Step Solar Maximum Power Point Tracking for Rapid Irradiance Tracking and Steady-State Losses Minimization

Francisco Paz and Martin Ordonez
Electrical and Computer Engineering Department
The University of British Columbia
Vancouver, BC, Canada
Email: {franciscopaz, mordonez}@ieee.org

***Abstract*—This paper develops the theory for an adaptive Maximum Power Point Tracking (MPPT) strategy to reduce extraction losses and other issues typically introduced by Perturb and Observe (P&O) algorithms. Three techniques to improve steady-state behavior and transient operation are discussed in detail: 1) idle operation on the Maximum Power Point (MPP), 2) irradiance direction change identification and 3) multi-level adaptive tracking step.**

**As a result, these strategies are combined to achieve superior overall performance while maintaining a simplicity of implementation. Two key elements which form the foundation of the techniques are discussed: the suppression of perturb oscillations at the MPP and the indirect identification of irradiance change through a current-monitoring algorithm. The Zero-oscillation, Adaptive-step Perturb and Observe (ZA-P&O) strategy is studied with simulation and validated with experimental results. The mechanism for power extraction gains is evident, making the combined techniques an excellent solution to enhance MPPT performance.**

## Nomenclature

| | |
|---|---|
| $direction$ | Flag to indicate the direction of the perturbation. |
| $e$ | Error signal, input of the PI controller. |
| $e_{Th}$ | Threshold for $e$ to trigger the tracking algorithm. |
| $FF$ | Fill Factor (or Form Factor). |
| $G$ | Amount of irradiance from the Sun in the PV panel. |
| $Idle$ | Flag to indicate the idle mode. |
| $i_{last}$ | Measured PV current in the last iteration. |
| $i_{mpp}$ | PV panel current at the MPP. |
| $i_{pv}$ | PV panel current at the operating point. |
| $i_{set}$ | Current set point, output of the PI controller. |
| $i_{Th}$ | Threshold for the change in $i_{set}$ to activate the algorithm. |
| $P_{last}$ | Measured power in the last iteration. |
| $T$ | Temperature of the PV panel. |
| $ToggleC$ | Counter for the number of toggles around the MPP. |
| $ToggleM$ | Maximum number of toggles around the MPP allowed before activating the idle mode. |
| $v_{mid}$ | PV voltage around which the MPPT oscillates in steady state. |
| $v_{mpp}$ | PV panel voltage at the MPP. |
| $v_{pv}$ | PV panel voltage at the operating point. |
| $v_{set}$ | Voltage set point, reference of the PI controller. |
| $V_{initial}$ | Initial voltage set-point for the MPPT strategy. |
| $V_{step}$ | Size of the perturbation step for the P&O strategy. |

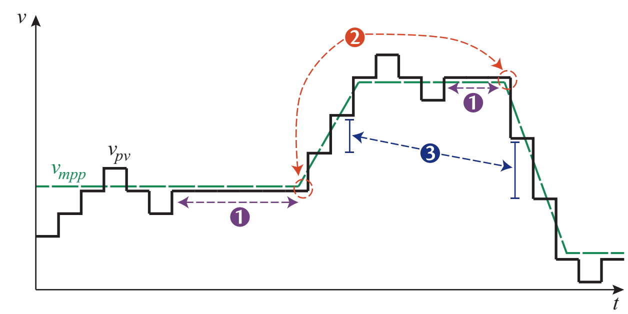


Fig. 1. Conceptual representation of the ZA-P&O combined MPPT strategies: efficiency maximized with no oscillation ❶, correct decision ❷ and step adjustment ❸ under changes in irradiance.

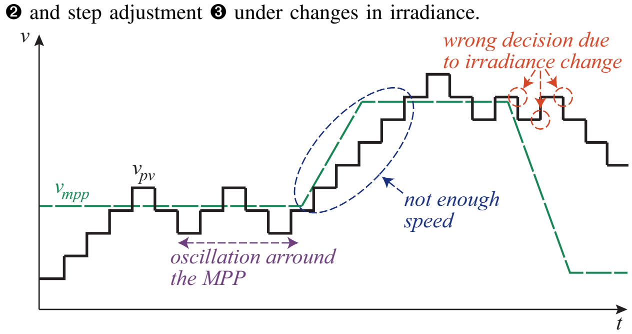


Fig. 2. Issues with P&O technique: oscillation in steady state, wrong tracking step and confusion during irradiance change.

## I. Introduction

Maximum Power Point Tracking (MPPT) for photovoltaic (PV) panels has seen many contributions in the past years [1] but some issues remain unsolved. Many techniques have been presented to track the Maximum Power Point (MPP) [2]; some have a very simple implementation but reduced efficiency, such as the Constant Voltage (CV), Fractional Open-Circuit Voltage (FOCV) and Fractional Short-Circuit Current (FSCI) methods, where the relationship between the open-circuit voltage/short-circuit current and the MPP voltage/current is assumed to be constant and independent of the weather conditions [2], [3]. Complex implementations achieve high performance by using a detailed model of the PV panel and additional measures of the irradiance (G) and temperature (T) [2], [4]–[6].The hill-climbing techniques, Perturb and Observe (P&O) and Incremental Conductance (InCon), are simple algorithms that can obtain high efficiency with a low computational cost and with no information about the particular PV to which they are connected and, for this reason, they have earned a predominant position amongst the MPPT algorithms. However, they both have similar issues regarding the losses in steady-state [7] and the identification and tracking of fast changing environmental conditions [8]–[10]. Recently, some strategies have been developed to overcome the confusion due to changes in G [11], [12].Opportunities to further improve steady-state behavior and provide an accurate tracking under rapidly changing G remain open, and are addressed in this work by combining three techniques.

In this paper, the theory for a MPPT strategy referred to as Zero-oscillation, Adaptive-step Perturb and Observe (ZA-P&O), which reduces losses in steady-state and improves tracking under rapid changes in G is developed. The losses are reduced by suppressing the oscillation around the MPP in steady-state, and are made possible by indirectly estimating a change in G through the error on a Proportional-Integral (PI) controller and the change in current in the operating point. Estimating the change enables the perturbation step to be adjusted in order to accurately track the changes in the MPP. The main advantages of this combined strategy are presented in Fig. 1 in comparison with the standard P&O in Fig. 2: 1) the efficiency in steady state is improved by suppressing the oscillation, 2) the confusion due to irradiance change is eliminated and 3) the step is adjusted for accurate tracking.

## II. PV System Model

The block diagram in Fig. 3 shows the implemented photovoltaic (PV) system; the PV panel is connected to a power converter that can be controlled to take more or less current ($i_{set}$). The PV panel voltage ($v_{pv}$) is regulated to the set point ($v_{set}$) by the $PI$ controller. As opposed to regular topologies for power converters, in this case the power converter will regulate the input voltage instead of the output, which is regulated by the load. The $v_{set}$ is determined by the proposed MPPT strategy by using information from the PV panel output current ($i_{pv}$), $v_{pv}$ and the error signal in the $PI$.

The equivalent circuit for a PV panel is presented in Fig. 4 [13], including the parasitic effects of the series resistor ($R_S$) and the shunt resistor ($R_{Sh}$). The current source represents the conversion of $G$ in electrical current, called photocurrent ($i_G$). For a solar cell, $i_G$ is proportional to $G$

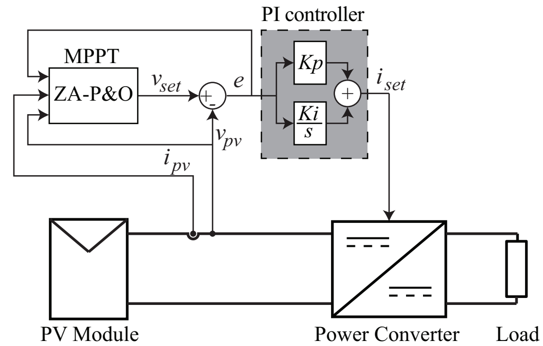


Fig. 3. Block diagram of the implemented photovoltaic (PV) system, the PV module is connected to a power converter to regulate the operation at maximum efficiency.

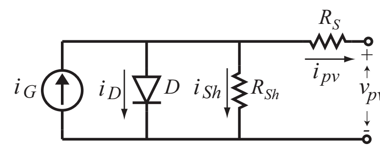


Fig. 4. Photovoltaic panel model including the parasitic effects of the series resistor ($R_S$) and the shunt resistor ($R_{Sh}$), the photocurrent ($i_G$) is proportional to the irradiance ($G$).

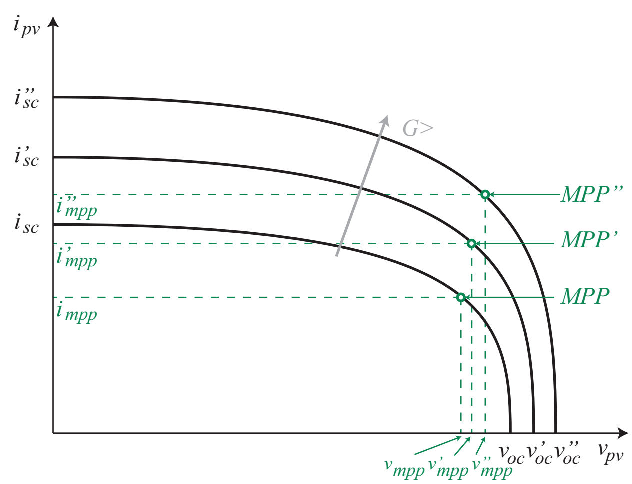


Fig. 5. Photovoltaic (PV) panel current as a function of the PV panel voltage, as a function of the irradiance ($G$); the Maximum Power Point current ($i_{mpp}$) is more sensible to changes in the irradiance than the voltage ($v_{mpp}$).

$$i_G \propto G. \tag{1}$$

The relationship between $i_{pv}$ and $v_{pv}$ is given by the following implicit expression [6]

$$i_{pv} = i_G - I_0[\exp\{\frac{q}{nkT}(v_{pv} + R_S i_{pv})\} - 1] - \frac{v_{pv} + R_s i_{pv}}{R_{Sh}} \tag{2}$$

where $I_0$ is the reverse saturation current of $D$, $q$ is the electron charge, $n$ is the diode factor, $k$ is Boltzmann's constant (in joules per kelvin), T is the PV panel temperature (in kelvin). The plots in Fig. 5 show the characteristic voltage/current curves for a PV panel, for different values of $G$. The MPP is the operating condition ($v_{mpp}$, $i_{mpp}$) that yields the maximum possible power for a given $G$. As $G$ changes, the MPP moves to different regions. As can be seen from Fig. 5, $i_{mpp}$ is more affected than $v_{mpp}$ by the change in $G$, therefore, it makes sense to implement the MPPT controller regulating $v_{pv}$.

## III. Proposed MPPT Strategy

The ZA-P&O MPPT strategy is based two key aspects: 1) detection of the steady-state operation and 2) determination of the direction and magnitude of the perturbation. In steady-state, the standard P&O algorithm will oscillate around the closest possible voltage (due to quantization of the voltage step) in three levels, as in Fig. 2. The ZA-P&O identifies this condition and establishes the operating point ($v_{set}$) in the closest value, as shown in Fig. 1. In this condition, called idle mode, the losses are minimized since the PV panel will always operate close to the MPP. When a change in $G$ is identified, using the error of the PI and the change in current, the direction and magnitude of the step is determined. This allows tracking to reactivate when it is needed and to establish an accurate step size based on the known slope, instead of toggling continuously as it is traditionally done.

The flow chart for the ZA-P&O is presented in Fig. 6. The strategy includes several tunable parameters, such as the thresholds for the current change and error ($i_{Th}$ and $e_{Th}$) and the number of oscillations around the MPP to establish the idle mode ($ToggleM$). Out of the special conditions established before, the algorithm works as a P&O. In the following paragraphs, details of the implementation of the different features are given.

### A. Idle mode operation

Traditional MPPT strategies search for the MPP by periodically changing the operating point of the PV panel and measuring the effects over the power or some other parameter [8], [9]. Since no way of identifying a change in the irradiance (and the corresponding displacement of the MPP) is included the MPPT strategies must keep perturbing the operating point even when the MPP has been found. This is reflected in a three-level operation condition shown in Fig. 2, where the operating point toggles around the closest voltage allowed by the discrete steps. The ZA-P&O MPPT strategy uses an indirect method to identify the changes in G, making it possible to eliminate this perturbation.

The proposed method identifies the operation around the MPP by counting consecutive changes in direction with a common middle point. When a step is introduced in $v_{set}$, if the step is the second in the same direction, the algorithm displaces the middle point ($v_{mid}$). The software computes one toggle and register it in the toggle counter ($ToggleC$) each time the set point returns to $v_{mid}$. The maximum number of toggles around $v_{mid}$ before activating the idled mode is set as a parameter ($ToggleM$) and is used to avoid confusion due to noise.

### B. Irradiance change identification

The PI controller ensures that the voltage is regulated with zero steady state error after each change in the voltage set-point ($v_{set}$), except when there is a change in $G$. Moreover, since an increment in $G$ always leads to a general increment in $i_{pv}$, $i_{mpp}$ and $v_{mpp}$ (and the opposite also holds true), it is possible to activate the MPPT algorithm in the correct direction, which is a great advantage over conventional MPPT algorithms.

When $G$ has a change that stabilizes before the next sample time of the MPPT algorithm (a step-like change), the PI controller will change the current to a new value to keep the voltage constant [3]. In this case, comparing $i_{pv}$ in between two consecutive steps (operating in idle mode) a step change in $G$ can be identified and the MPPT tracking is reactivated.

When the change in $G$ has a ramp-shape (a constant slope through time), the PI controller cannot reduce the error ($e$) to zero. In this case, the error will be [12]

$$e \propto \frac{\alpha}{K_i} \tag{3}$$

where $\alpha$ is the slope of the change in $i_{pv}$, which results from the slope change in $G$, and where $K_i$ is the integral component of the PI controller. Once again, the change in $G$ has been identified and the correct direction for the next change can be obtained. The use of this identification method has the advantage of being independent of the step perturbation introduced by the strategy, so complex decoupling algorithms are not needed.

### C. Step adaptation

As discussed above, when $G$ changes with a step form, the correct direction to start the tracking of the MPP is obtained, but this is not enough when the irradiance changes with a slope. If the slope is too small, the MPPT may detect the change and introduce a step that will lead the operating point far away from the MPP. If the slope is too steep, the steps may not be large enough to track the MPP. Since the magnitude of the slope can be identified from (3), the magnitude of the change in $i_{pv}$ that results from the change in $G$ is known as

$$\Delta i_{pv} = K_i e \Delta t \tag{4}$$

where $\Delta t$ is the sample time of the MPPT strategy. As can be seen, from the measurement of $e$ and the knowledge of $K_i$ and $\Delta t$ it is possible to know the change in $i_{pv}$, proportional to the change in $G$. In this condition, we can adjust the step in proportion to the change in the $G$. The value of the proportionality constant depends on the PV panel.

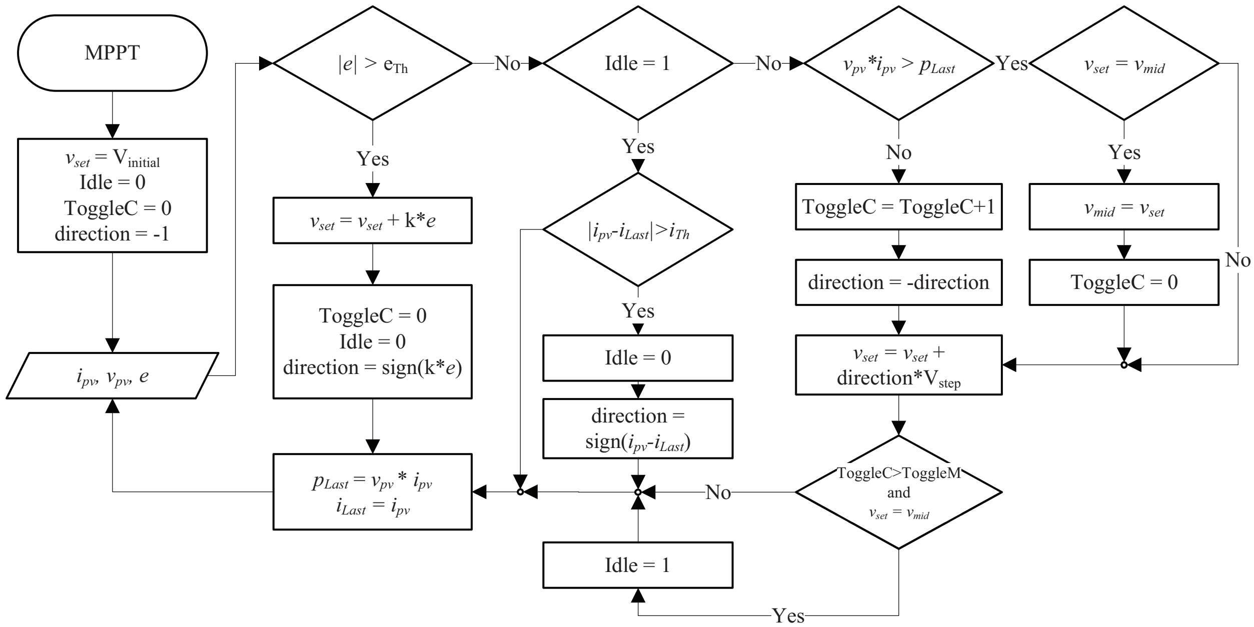


Fig. 6. Flow Chart for the ZA-P&O MPPT strategy. This strategy includes an idle mode for the steady-state, slope detection and adaptive step.

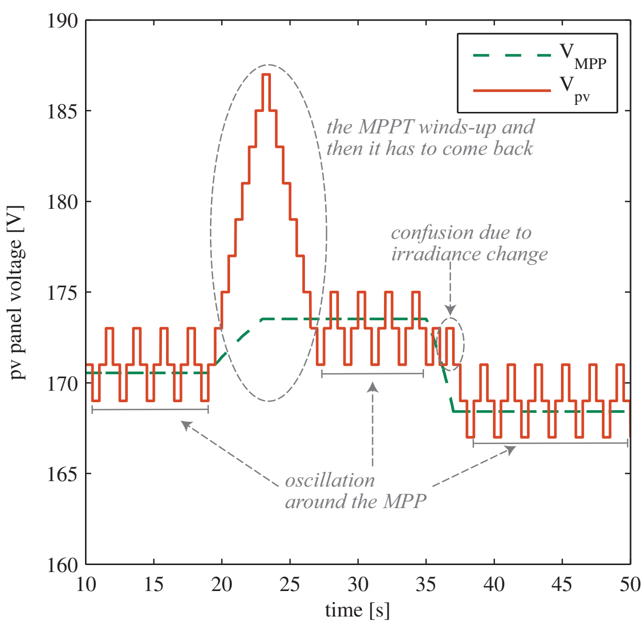


Fig. 7. Standard P&O MPPT pitfalls: a) irradiance change begins during a tracking step-up leading to MPPT wind-up, b) confusion due to irradiance reduction leads to accidental sustained toggling and c) oscillation around the MPP reduces efficiency.

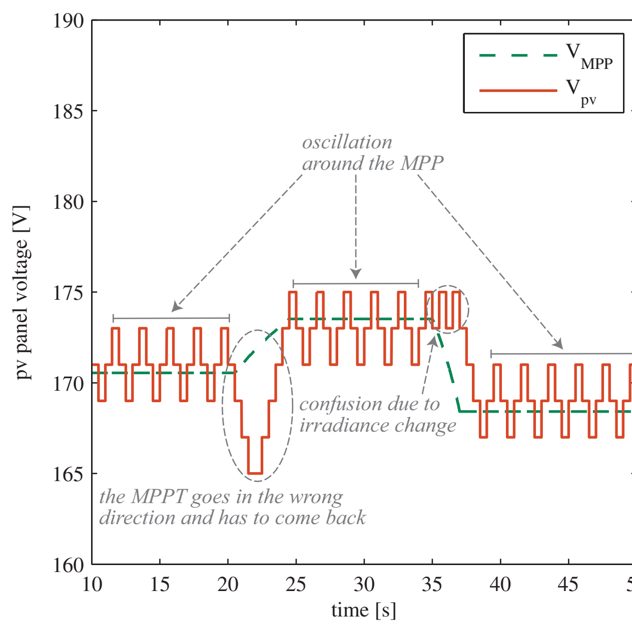


Fig. 8. Standard P&O MPPT pitfalls: a) irradiance change begins during a tracking step-down leading to MPPT going in the wrong direction, b) confusion due to irradiance reduction leads to accidental sustained toggling and c) oscillation around the MPP reduces efficiency.

## IV. Simulation and Experimental Results

### A. Simulations

This section presents the results of the computer simulation for both the ZA-P&O MPPT and the standard P&O for a trapezoidal irradiance (G) profile. The model is composed of a PV panel that can be configured to perform with the desired characteristics, a PI controller to regulate the voltage of the PV panel, and the MPPT to determine the operating point. The output of the PI controller sets the current in the PV panel.

The PV panel is configured to have 200 V open-circuit voltage and 5 A short-circuit current, with a Fill Factor (FF) of 0.8 at standard test conditions (STC, 1 kW/m$^2$ and 25 °C). The MPPTs are configured with the same voltage step for

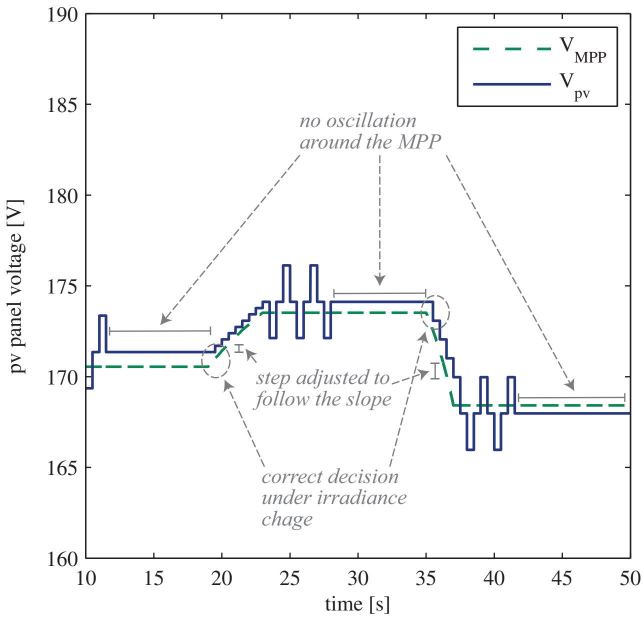


Fig. 9. ZA-P&O strategy improvements: a) the correct direction is identified, b) the change is accurately tracked and c) oscillation and efficiency reduction are suppressed.

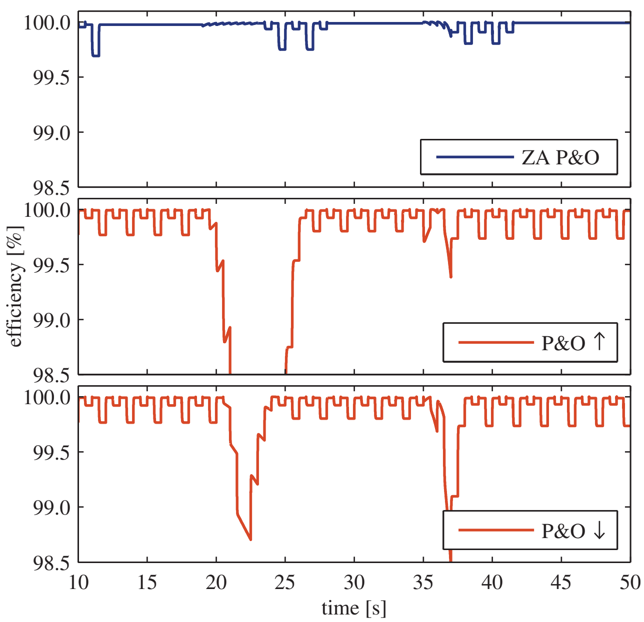


Fig. 10. Efficiency of the PV panel for the ZA-P&O (blue) and the standard P&O (red) when the slope starts in the falling edge (P&O ↓) and in the raising edge (P&O ↑).

the P&O part and the same sampling period. The sampling period of the MPPT is established in $0.5$ s and the fixed voltage step is $1$ V. The testing profile starts at $0.8$ kW/m$^2$, at $t = 20$ s it starts increasing with a slope of $0.1$ kW/m$^2$s. When it reaches $1.2$ kW/m$^2$ it stops and waits for $11$ s and then it starts decreasing with a slope of $0.3$ kW/m$^2$s until it reaches $0.6$ kW/m$^2$. Then it remains constant until the end of the simulation. To illustrate the error in tracking for the standard P&O, two cases were studied, a) slope was started during a falling edge and b) during a raising edge of the MPPT. The input signals to the MPPT are $v_{pv}$, $i_{pv}$ and the error of the PI controller. When the standard P&O is tested, the error is not used. For the simulations, the threshold level of the current and the error ($i_{Th}$ and $e_{Th}$) are set to zero, since there is no noise in this environment.

The results of the simulation for the standard P&O are displayed in Figs. 7 and 8, while the results for the ZA-P&O MPPT are presented in Fig. 9. The standard P&O keeps going in the same direction it was going when the irradiance changed (since it detects an increase in power) even when it is going in the incorrect direction. When the irradiance decreases, it starts toggling in the same position, since any step produces a decrement in power. This deviation from the correct direction can lead to a large loss in performance, since real profiles can have slopes for extended periods of time. More than that, the standard MPPT algorithm is unable to adjust the tracking step to different $G$ slopes, this leads to an algorithm that, even when it goes in the correct direction, may drift from the MPP because of the wrong step selection.

The ZA-P&O MPPT strategy produces far better results. The idle operating mode allows the PV panel to operate in a smooth way when there is no need to keep tracking. When a change occurs in G, the strategy clearly identifies the correct direction to move the operating point and adjust the step size to provide a close tracking of the MPP. The effectiveness of the identification does not depend on the moment the irradiance slope starts.

The efficiency of the tracking is shown in Fig. 10, where the blue curve represents the ZA-P&O and the two red ones represent the standard P&O. It is evident how the ZA-P&O improves the overall performance: 1) in steady-state, the efficiency remains constant and close to $100\%$ instead of oscillating periodically, 2) the correct direction is determined and 3) the step is adjusted; thus the efficiency remains high even during the transient, whereas the standard P&O leads to drops in efficiency.

### *B. Experimental Results*

Experimental results are shown in Fig. 11 for the proposed strategy and in Figs 12 and 13 for the standard P&O when the slope starts at a falling edge and a raising edge respectively. The benefits of the ZA-P&O are evident in the experimental curve, when compared with the standard P&O. The oscillation is removed and the step is given in the correct direction and magnitude, evidenced by the fast re-establishment of the idle mode after the irradiance slope ends. The standard P&O show the same issues as in the simulation. Some error is present due to noise, but proper filtering can help to minimize it.

As in the simulations, the standard P&O strategy drifts away from the MPP when the irradiance changes with a slope and the error increases with time. Keeping the oscillation around the MPP in the idle condition increases the probability of

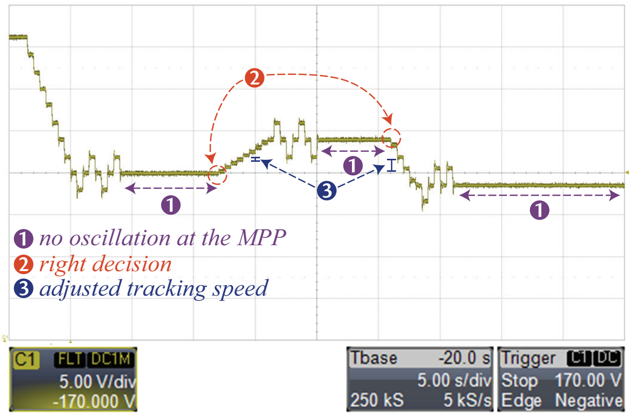


Fig. 11. Experimental capture of the ZA-P&O MPPT strategy for the same irradiance profile as in the simulation.

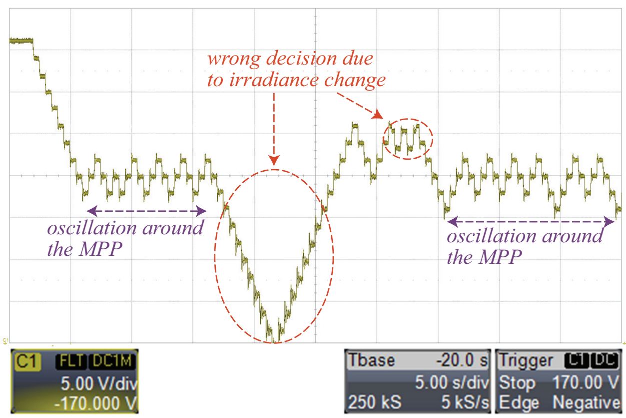


Fig. 12. Experimental capture of the standard P&O when the irradiance slope starts in a falling edge of the MPPT.

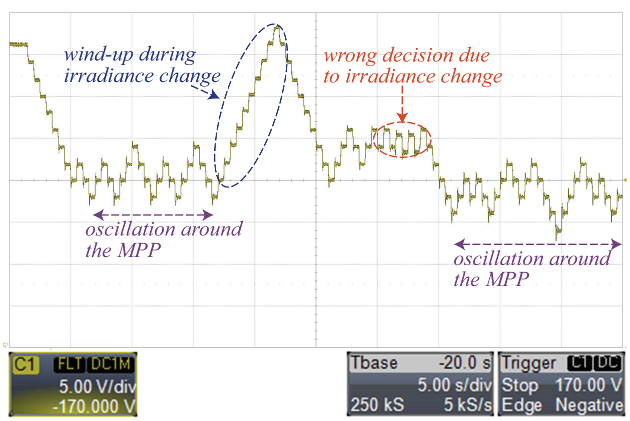


Fig. 13. Experimental capture of the standard P&O when the irradiance slope starts in a raising edge of the MPPT.

making a mistake due to the noise in the measurement, as is demonstrated in Fig. 12, where the P&O process reaches the MPP during the first stage and works with three levels but suddenly drifts away and returns. The ZA-P&O algorithm benefits from the removal of this perturbation to enable a clearer measure of the change in $G$.

## V. Conclusions

The theory for Zero-oscillation, Adaptive-step Perturb and Observe (ZA-P&O) Maximum Power Point Tracking (MPPT) strategy for solar photovoltaic (PV) panels was presented in this work. This combined strategy reduced steady-state losses and improved transient behavior during fast irradiance changes, while maintaining a similar implementation complexity. Enhanced behavior resulted from the combination of three techniques: 1) idle operation when steady-state is reached, 2) correct irradiance change identification and 3) multi-level adaptive tracking step. The idle operation was possible due to the identification of the irradiance change, through a current monitoring algorithm. The adaptive tracking speed minimized error during a fast change in irradiance. The proposed combined techniques were studied with simulations and validated through experimental results. The overall performance improvements, both in steady-state and during fast irradiance change, provide solid evidence of the benefits of the combined techniques.

## References

[1] M. de Brito, L. Galotto, L. Sampaio, G. de Azevedo e Melo, and C. Canesin, "Evaluation of the main mppt techniques for photovoltaic applications," *IEEE Trans. Ind. Electron.*, vol. 60, no. 3, pp. 1156 –1167, march 2013.

[2] B. Subudhi and R. Pradhan, "A comparative study on maximum power point tracking techniques for photovoltaic power systems," *IEEE Trans. Sustainable Energy*, vol. 4, no. 1, pp. 89 –98, jan. 2013.

[3] M. Masoum, H. Dehbonei, and E. Fuchs, "Theoretical and experimental analyses of photovoltaic systems with voltageand current-based maximum power-point tracking," *IEEE Trans. Energy Convers.*, vol. 17, no. 4, pp. 514 – 522, dec 2002.

[4] J. Blanes, F. Toledo, S. Montero, and A. Garrigos, "In-site real-time photovoltaic i-v curves and maximum power point estimator," *IEEE Trans. Power Electron*, vol. 28, no. 3, pp. 1234 –1240, march 2013.

[5] T. Esram and P. Chapman, "Comparison of photovoltaic array maximum power point tracking techniques," *IEEE Trans. Energy Convers.*, vol. 22, no. 2, pp. 439–449, 2007.

[6] N. Mutoh, M. Ohno, and T. Inoue, "A method for mppt control while searching for parameters corresponding to weather conditions for pv generation systems," *IEEE Trans. Ind. Electron.*, vol. 53, no. 4, pp. 1055 –1065, june 2006.

[7] C. Sullivan, J. Awerbuch, and A. Latham, "Decrease in photovoltaic power output from ripple: Simple general calculation and the effect of partial shading," *IEEE Trans. Power Electron*, vol. 28, no. 2, pp. 740 –747, feb. 2013.

[8] M. Elgendy, B. Zahawi, and D. Atkinson, "Assessment of the incremental conductance maximum power point tracking algorithm," *IEEE Trans. Sustainable Energy*, vol. 4, no. 1, pp. 108 –117, jan. 2013.

[9] M. Elgendy, B. Zahawi, and D. Atkinson, "Assessment of perturb and observe mppt algorithm implementation techniques for pv pumping applications," *IEEE Trans. Sustainable Energy*, vol. 3, no. 1, pp. 21 –33, jan. 2012.

[10] S. Kjaer, "Evaluation of the "hill climbing" and the "incremental conductance" maximum power point trackers for photovoltaic power systems," *IEEE Trans. Energy Convers.*, vol. 27, no. 4, pp. 922 –929, dec. 2012.

[11] D. Sera, R. Teodorescu, J. Hantschel, and M. Knoll, "Optimized maximum power point tracker for fast-changing environmental conditions," *IEEE Trans. Ind. Electron.*, vol. 55, no. 7, pp. 2629 –2637, july 2008.

[12] R. Kadri, J.-P. Gaubert, and G. Champenois, "An improved maximum power point tracking for photovoltaic grid-connected inverter based on voltage-oriented control," *IEEE Trans. Ind. Electron.*, vol. 58, no. 1, pp. 66 –75, jan. 2011.

[13] A. Luque and S. Hegedus, *Handbook of Photovoltaic Science and Engineering*. Wiley, 2003.